Role of three-dimensional transesophageal echocardiography in cardiac myxomas: an imaging challenge

Bandar Alamro,[1,2] Valeria Pergola,[3] Abdalla Eltayeb,[1,4] Amal Alshammari,[1] Naji Kholaif,[1,2] Ahmad Alhamshari,[2] Mohammed Al Admawi,[1] Shamayel Mohammed,[1] Feras Khaliel,[1] Domenico Galzerano[1,2]

[1]The Heart Centre, King Faisal Specialist Hospital and Research Center, Riyadh, Saudi Arabia; [2]College of Medicine, Alfaisal University, Riyadh, Saudi Arabia; [3]Department of Cardio-Thoraco-Vascular Sciences and Public Health, University of Padua, Italy; [4]Division of Cardiovascular Medicine, Krannert Cardiovascular Institute, Indiana University School of Medicine, Indianapolis, IN, USA

Correspondence: Abdalla Eltayeb, The Heart Centre, King Faisal Specialist Hospital and Research Center, Riyadh, Saudi Arabia.
E-mail: abdullaheltayeb2002@gmail.com

Key words: cardiac myxomas, transesophageal echocardiography, 3-dimensional echocardiography, magnetic resonance imaging.

Contributions: all the authors made a substantive intellectual contribution, performed part of the experiments. All the authors read and approved the final version of the manuscript and agreed to be accountable for all aspects of the work.

Conflict of interest: the authors declare that they have no competing interests, and all authors confirm accuracy.

Ethics approval and consent to participate: this study project has been conducted in accordance with the ethical principles contained in the Declaration of Helsinki (2000), the ICH Harmonized Tripartite Good Clinical Practice Guidelines, the policies and guidelines of the Research Advisory Council (RAC) of the King Faisal Specialist Hospital and Research Center, and the laws of Saudi Arabia. As this was a retrospective study and did not involve any direct contact with patients or their families and did not pose more than a minimal risk to patients, a waiver of informed consent was approved by RAC.

Informed consent: not applicable.

Patient consent for publication: not applicable.

Availability of data and materials: the datasets used and/or analyzed during the current study are available from the corresponding author on reasonable request.

Funding: none.

Received: 3 September 2023.
Accepted: 12 September 2023.
Early view: 19 September 2023.

Monaldi Archives for Chest Disease 2024; 94:2768
doi: 10.4081/monaldi.2023.2768

Abstract

Nowadays, the diagnosis of cardiac myxomas (CM), particularly the histological types, remains a challenge. Two-dimensional (2D) transthoracic (TT) and transesophageal (TEE) echocardiography (ECHO) represent the first steps in the imaging pathway. 3D ECHO, implemented in imaging practice, appears to be an emerging diagnostic technique that overcomes some of the limitations of 2D ECHO while integrating the information provided by magnetic resonance (MRI). However, its role in the imaging arena is still debatable. Analyzing 17 myxomas in 13 patients, the study uncovers a diverse anatomical spectrum. Classical CM morphology is a minority, with most myxomas being sessile and originating from unexpected locations (right ventricular outflow tract and left atrial appendage). Texture and size variations are also noted. Comparing imaging, 2D TEE outperforms 2D TT in visualizing anatomical features, especially attachment types. 3D TEE confirms 2D TT findings and offers more detailed assessments, identifying peduncles missed in four cases by 2D TEE. Two small recurrent myxomas were exclusively detected by 3D TEE, not by 2D TEE or MRI. Two patients have papillary myxomas, and one has an embolism. Another patient with a solid myxoma also suffers an embolism, with a clot found at the apex during surgery. Our study showed that CM has a wide anatomical spectrum beyond the typical features, making the diagnosis challenging. Therefore, a multimodality imaging approach is essential for distinguishing CM from other cardiac masses and differentiating myxoma histological types. These findings stress the importance of incorporating 3D ECHO alongside other imaging techniques for a comprehensive evaluation.

Introduction

Nowadays, the diagnosis of cardiac myxomas (CM), particularly of the histological types, remains a challenge [1-7]. Two-dimensional (2D) transthoracic (TT) and transesophageal (TE) echocardiography (ECHO) represent the first steps in the imaging pathway [5,8,9]. Even though ECHO has an excellent sensitivity for CM diagnosis, the specificity is still modest due to a wide differential diagnosis [1-9]. In the imaging scenario, three-dimensional (3D) TE ECHO, thanks to technological advances allowing fast reconstruction of realistic anatomic images of cardiac structure, has been implemented in routine imaging practice [10-12]. Currently, both TT ECHO and TE ECHO transducers can generate 3D images. However, 3D TE ECHO, which provides images of higher quality compared to 3D TT ECHO, is the modality capable

of allowing for detailed anatomical imaging [10,11]. In the cardiac tumor imaging scenario, it appears to be an emerging diagnostic technique that overcomes some of the limitations of 2D ECHO while integrating the information provided by magnetic resonance imaging (MRI) and cardiac computed tomography (CT) [12-21]. However, its role in the imaging arena is still debatable.

In the imaging pathway of cardiac masses and myxomas, the type and site of attachment (pedunculated or sessile), surface characteristics (smooth and bosselated versus irregular and fimbriated), and echotexture (presence of hemorrhagic areas and calcification showing different echotextures, homogeneous *versus* heterogeneous/non-homogeneous) hold paramount importance [5,8,9,12,21]. The correct visualization of these morphological features can lead to the diagnosis of the presence of myxomas versus other intracardiac masses, as well as the specific type of myxoma (solid or polypoid versus papillary or myxoid). Two types of myxomas in macroscopic examination have been identified: solid or polypoid myxomas with a round shape and a smooth surface usually attached to the interatrial septum (IAS) and papillary myxomas characterized by an asymmetrical and soft shape with an irregular surface attached to various locations. The latter type has been shown to have a higher risk of systemic embolism, either due to the irregular or friable villous surface of the tumor or through thrombus formation. However, thrombus formation may also be present in the solid type [1-7].

The majority of CM are polypoid and pedunculated (rarely sessile), presenting as round or ovoid tumors with smooth, glistening, or slightly lobulated surfaces, and a short broad base. Polypoid myxomas are typically compact, solid tumors with little tendency for spontaneous fragmentation. Less commonly detected are papillary myxomas, which exhibit multiple thinner or thicker villous, finger-like extensions and possess a soft, gelatinous structure that is highly susceptible to fragmentation, erosion, and embolization. Multimodality imaging is required to accurately detect recurrent myxomas by identifying their anatomical features and perfusion; however, each imaging modality has its limitations [5,8,9,13-21]. While 2D TT ECHO and TE ECHO are the preferred techniques for initial assessment, the detection of the type and site of attachment and a detailed evaluation of tumor echotexture and surface characteristics are not always accurate or feasible. Previous reports have demonstrated that 3D ECHO, allowing electronic scanning through unconventional and unrestricted 2D cross-sectional planes likewise an electronic autoptic sectioning, offers additional value in assessing morphological features of CM [8,9,13-18]. MRI is considered the gold standard for diagnosing cardiac tumors and myxomas, enabling not only the detection of intracardiac masses but also the evaluation of various parameters including tissue characterization, edema, iron content, perfusion, enhancement, and fat saturation/suppression [20,21]. However, it also presents some technical limitations and might not always detect anatomical features like tiny stalks [5,13-21]. In the context of CM imaging, 3D TE ECHO, providing detailed real-time anatomical imaging and unique electronic scanning, may play an emerging role as a key adjunctive modality, especially when anatomical clarity is lacking with 2D ECHO and advanced surgical planning is required [10,11,16,17]. Furthermore, the use of anatomical imaging and an anatomy-based vocabulary, which is better understood by cardiac surgeons and multimodality imagers, positions 3D TE ECHO as the echocardiographic modality that can enhance communication within the Heart Team [10,11]. By bridging the gap between 2D ECHO and anatomy and adding more detailed information on the morphologic features, its utilization could represent a missing link in myxoma imaging [10-19].

Materials and Methods

Study design

This was a retrospective observational study that included patients who had surgery and had a pathological diagnosis of CM. Patients' demographics, symptoms, presence of embolism, imaging performed (2D TT ECHO, 2D TE ECHO, 3D TE ECHO, MRI), surgery, and histological type of myxomas were all studied.

Echocardiography

2D and 3D TT and TE ECHO data were reported. iE33, EPIC 7C, and EPIC CVS 3D system (Philips Medical Systems, Andover, MA, USA) and GE E90, E95 echocardiographic machines equipped with 2D and 3D TE echocardiographic imaging have been used. All images were stored digitally and were offline reviewed on the machine and on Qlabs software (Philips Medical Systems) and EchoPAC (GE HealthCare, Chicago, IL, USA). Electronic 2D scanning of the 3D anatomical and surgical view has been performed to detect the size and location of the tumor, the presence or absence of a stalk, the smoothness of the surface (smooth vs lobulated), and the presence or absence of papillary excrescences, echotexture described as similar or different to the myocardium (hypoechogenic or hyperechogenic) and as homogenous or heterogeneous according to the absence or presence of areas with different echotexture.

Magnetic resonance

Cine steady-state free procession (SSFP), first-pass perfusion, and late gadolinium enhancement (LGE) will be reviewed and analyzed. T1-weighted, T2-weighted, and T2-fat-saturated sequences acquired in two planes orientated will be examined. Cine SSFP imaging sequences, acquired in standard cardiac imaging planes, provide an accurate assessment of the location, attachment site and functional impact of myxomas. On cine SSFP sequences, myxomas typically appear hyperintense compared with normal myocardium and hypointense compared with the blood pool. Cine SSFP imaging is of particular value in the functional assessment of atrial myxomas, as lesions here can be highly mobile.

Results

We have retrospectively collected 17 myxomas in 13 patients, 9 females, mean age 40 range 18-71 years (Table 1).

Case #1

A 42-year-old female with a history of diabetes mellitus, hypertension, and a prior stroke, was admitted to the hospital due to symptoms suggestive of a stroke. Subsequent brain imaging through both CT and MRI indicated findings consistent with chronic ischemic injury. In the process of investigating the stroke, comprehensive cardiac evaluations were conducted, including TTE revealed the presence of a mass attached to the left atrium (LA) attached to the IAS; the mass size was 18×21 mm. 2D and 3D TE ECHO showed a large mobile mass seen in the LA measured at least 18×21 mm attached to the IAS, not causing significant obstruction to flow across the mitral valve. The mass was surgically resected, and the pathology showed the mass to have solid characteristics, organized in cord-like formations with no vascular structures within the mass.

Case #2

A 57-year-old female hypertensive, diabetic, with a history of previous cerebrovascular accident (CVA), *in sinus* rhythm, underwent a TT ECHO to detect the source of embolism following a newly diagnosed CVA. The exam showed a large mobile mass in the LA (size 1.7×3 cm), with irregular shape and borders and with a nonhomogeneous echo structure. The mass seemed to originate from the right inferior pulmonary vein (RIPV) or from the basal IAS. Cardiac magnetic resonance (CMR) showed a mass in the LA, isointense on T1 images, and heterogeneous enhancement on late gadolinium. It was unable to identify a peduncle or clearly

Table 1. Data and characteristics of the study population.

Case	Age/Gender	Symptoms	Echo findings 2D TTE, 2D/3D TEE.	Histology
1	42/F	Yes (brain infarcts)	2D TTE: large mobile mass seen in the left atrium measured at least 1.8×2.1 cm attached to the IAS, not causing significant obstruction to flow across the mitral valve 2D 3D TEE: pedunculated mass attached to the interatrial septum	Solid
2	57/F	Yes (brain infarcts)	2D TTE: mobile mass in the left atrium (size1.7×3cm), with irregular shape with a nonhomogeneous echotexture. The mass seemed to originate from the RIPV or from the basal IAS 3D TEE: attached by a peduncle to the inferior atrial septum near to the opening of right inferior pulmonary vein	Papillary
3	53/M	No	2D TTE: the mass is attached via a pedicle to the interatrial septum in the region of fossa ovalis (1.5×4.2 cm) 2D 3D TEE: large mass attached to interatrial septum on the left atrial side more anteriorly just behind the aortic valve	Solid
4	31/F	Yes (chest pain)	3D/2D TTE: sessile attachment to the lateral atrial wall. The atrial mass is large and has irregular surface, fimbriated (fluffy appearance)	Papillary
5	33/F	No	2D TTE: multi-lobulated masses seen in RA. Septal attachment could not be confirmed but it is likely attached to the septal 3D TEE: multi-lobulated mass seen in the right atrium that seems attached to the interatrial septum close to SVC and aorta; at the same level of the interatrial septum there is another small mass on left atrial sid; another small mass seen on the close to the opening of LAA; small mass attached close to the posteromedial commissure and P3 scallop of the mitral valve. The RA mass partially protrudes through tricuspid valve during diastole with no significant obstruction to flow	Solid
6	65/F	No	2D TTE: regular border mass is arising from the atrial septum (size 2.1×4 cm) 2D 3D TEE: sessile attachment to the IAS. With some area of heterogeneity with regular smooth surface. Size 2.2×4.2 cm	Solid
7	46/F	Yes (SOB/ palpitations)	2D TTE: large and highly mobile mass in the LA, attached to the interatrial septum at the fossa ovale; the mass measures ~6×3.3 cm and protrudes across the MV in diastole into the LV inflow causing severe obstruction to flow. Two large central hypoechogenic areas noted within the mass may represent central necrosis 2D 3D TEE: huge mass, pedunculated, attached to the interatrial septum. Size 60×33 mm	Solid
8	46/M	No	2D TTE: pedunculated, attached to the interatrial septum 2D TEE pedunculated, attached to the interatrial septum	Solid
9	71/F	Severe aortic stenosis	2D TTE: no mass by TTE3D TEE: sessile mass attached to the left side of fossa ovalis (size 1.9×1.2 cm) with irregular shape and soft echo structure	Solid
10	39/M	No	2D TTE: mobile mass 14×24 mm attached to the interatrial septum 2D 3D TEE: mass with heterogeneous texture, well-defined borders, with on the top fimbriated edges, attached to the atrial wall	Solid
11	19/F	No	2D TTE: large rounded mobile mass (2×2 cm) with a short thick pedicle just below aortic valve but no sub-aortic obstruction 2D 3D TEE: large rounded mobile mass with a short thick pedicle attached to the RVOT just below aortic valve	Solid
12	18/M	No	2D TTE: large RA myxoma measuring 3.5×3.0 cm attached to the IAS with no significant obstruction 2D 3D TEE: a large mobile, with well delineated margins and heterogenous mass attached to the RA wall just anterior to the mouth of the IVC, measuring ~4×3 cm in diameter and partially protruding into the TV inflow and partially obstructing the inflow of the coronary sinus. No obstruction to IVC, SVC or TV inflow	Solid
13	48/F	No	2D TTE: round large mass (1.9×1.6 cm) attached to fossa ovalis, smooth surface homogeneous likely attached by a peduncle not seen clearly by TTE 2D 3D TEE: round large sessile mass (1.9×1.6 cm) attached to fossa ovalis	Solid

F, female; M, male; 2D, two-dimensional; 3D, three-dimensional; TTE, transthoracic echocardiography; TEE, transesophageal echocardiography; IAS, interatrial septum; RIPV, right inferior pulmonary vein; RA, right atrium; LA, left atrium; LAA, left atrium appendages; LV, left ventricle; IVC, inferior vena cava; SVC, superior vena cava; TV, tricuspid valve; RVOT, right ventricular outflow tract; MV, mitral valve; SOB, shortness of breath.

identify the site of attachment. No opacification of the mass was found by angiography. A cardiac CT scan also found a mass in the LA close to the RIPV, but again, it failed to characterize its attachment. A TE ECHO was then performed. It demonstrated the presence of a mobile mass protruding into the RIPV, without being able to correctly identify its origin. Careful assessment did not reveal other masses in LA and LA appendages (LAA). Further 3D acquisition was performed. By using 2D cutting planes on the 3D volume, the mass was sectioned in the different planes by the blue plane of the section, and we were able to identify the attachment of the mass as a tiny peduncle to the atrial floor at the base of the IAS close to the opening of RIPV. Surgical resection revealed a reddish jelly mass (size 3×3 cm) with a soft consistency attached to the atrial floor at the base of the IAS close to the RIPV. Pathological evaluation confirmed the diagnosis of myxoma [16].

Case #3

A 53-year-old male with a prior history of colorectal cancer underwent a routine abdominal CT scan to monitor his condition's progression. Unexpectedly, the scan revealed a mass in the LA near the mitral valve. Further 2D TT ECHO showed a mass attached *via* a pedicle to the IAS in the region of fossa ovalis sized 1.5×4.2 cm. 2D and 3D TE ECHO confirmed the TT ECHO findings and imaged the mass to be ovoid, measuring 23×20 mm, attached to the IAS by a thick peduncle attachment. A cardiac MRI was subsequently demonstrated a mass lesion sized at 2.3×1.8 cm attached to the atrial septum by a pedicle; the mass displayed increased signal intensity in short tau inversion recovery (STIR) and T1 sequences. contrast-enhanced sequences showed limited enhancement during perfusion and delayed phases. Pathology found a solid type myxoma.

Case #4

A 31-year-old female referred from local hospital with a diagnosis of left atrial mass for further evaluation. 3D/2D TT ECHO showed sessile attachment to the lateral left atrial wall that was confirmed at 2D TE ECHO (Figure 1). The atrial mass was large in size and had an irregular surface, fimbriated (fluffy appearance). At surgery, a gelatinous, very fragile mass attached to the roof of LA matching the imaging features was found and resected. Pathology examination found a papillary-type myxoma.

Case# 5

A 33-year-old female who underwent left atrial myxoma resection was found to have on a follow-up TT ECHO a large multilobular mass in the right atrium (RA). The RA mass was partially protruding into the tricuspid valve (TV) during diastole with no significant obstruction to flow. It was not possible to correctly detect the type of insertion of the tumor and no other masses were found. The patient was not aware of other occurrences of CM in family members. Further 2D TE ECHO showed two multi-lobulated masses in RA: one bigger (measuring around 4×3 cm, difficult to correctly size for its asymmetric morphology) attached by a peduncle to the superior lateral RA wall and one smaller attached by a stalk to the inferior RA wall. A remnant likely a suture was seen on the right side of the fossa ovalis; two additional masses were detected in the LA: i) a small (size 0.7×1.4 cm) sessile mass on the left atrial side of the IAS close to the scar of the previous surgery; ii) a small sessile (size 0.6×0.8 cm) mass attached to the mitral annulus close to the posteromedial commissure and P3 scallop of the posterior leaflet of the mitral valve. 3D TE ECHO allowed an anatomical imaging to identify two pedunculated right atrial masses and three sessile LA mass-

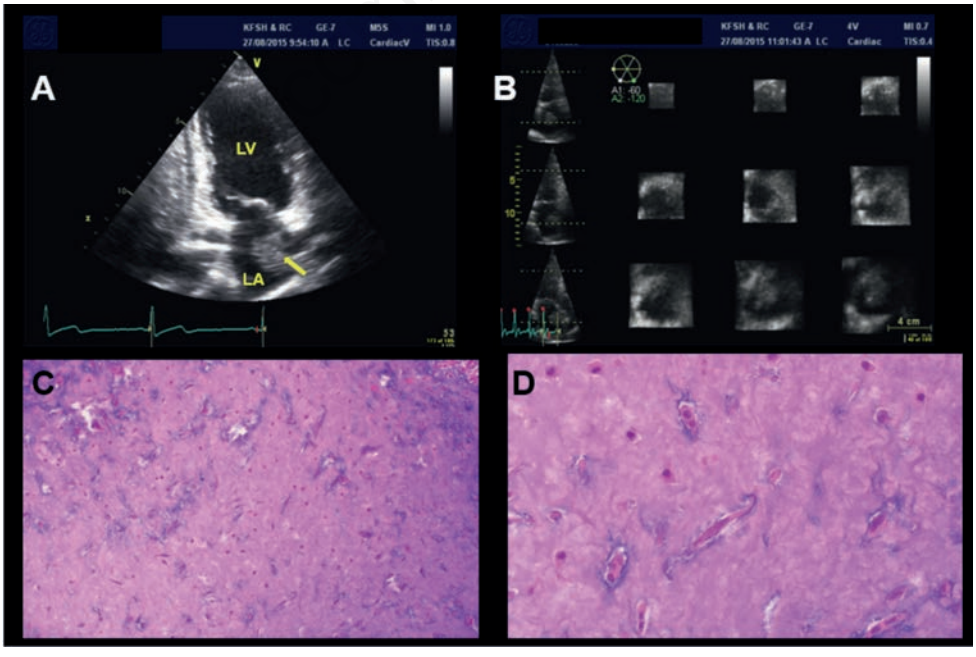

Figure 1. Case #4. A) Transthoracic echocardiography image showing a 2-chamber apical view with LA myxoma; B) 3D echocardiography volume sectioned at different levels showing left atrial myxoma; C,D) histological examination showing 4 acid-mucopolysaccharide-rich myxoid matrix with polygonal stromal cells scattered throughout papillary myxoma with single cell predominant subtype; the single myxoid cells were scattered.

es: i) one on the left side of the IAS close to the previous resection area; ii) one at the opening of the LAA and one on the mitral annulus in the area of the posterior commissure of the mitral valve. MRI multifunctional assessment cine, tissue characterization with T2-weighted edema imaging with fat saturation and first pass Gadolinium perfusion imaging and late enhancement imaging identified and showed perfusion of two masses in the RA with the pedicles, one mass on the LA side of IAS, and one mass on the mitral annulus close to mitral valve posterior commissure; however, it was not able to detect the small mass close to the LAA even after careful review by an expert reader.

The patient underwent reoperation through a biatrial approach; two lesions were found in the RA; one multilobular with two consistencies, one solid and one myxomatous, both connected by a thick pedicle to the right atrial wall superiorly and laterally. This one was resected with the underlying attachment to the RA; another separate lesion with a separate pedicle and attachment to the right atrial wall more inferiorly was also detected; it was also resected with the adjoining atrial tissue. Three lesions were found in the LA; one, about 1 cm in diameter, close to the scar for the last surgery, and also another two, smaller in size; one close to the opening of the LAA and one close to the posterior commissure of the mitral valve. The mitral valve was slightly involved during the resection of the lesion from the valvular annulus and was repaired by 4-0 Prolene sutures. Five specimens were sent to pathology; all of them, upon histopathologic study, were consistent with benign CM. No major clinical criteria are suggestive of Carney Syndrome (skin, conjunctiva, and lips lentigines, subclinical hypercortisolism, and nodular thyroid changes) except CM and no mutations of the *PRKAR1A* gene were found. After 18 months follow-up, no recurrences have been detected [17].

Case #6

A 65-year-old female patient with a medical history of diabetes, hypertension, and a previous myocardial infarction, presented to a local hospital with symptoms of pneumonia. During her workup, she was incidentally found a mass within the LA by ECHO. For this reason, she was referred to our center. 2D TT ECHO confirmed the presence of the left atrial mass; however, it was not possible to clearly identify the attachment. A subsequent 2D and 3D TE ECHO was able to demonstrate the sessile attachment to the IAS. A surgical resection was done to confirm the echo findings. Pathology found the mass to be a solid myxoma.

Case #7

A 46-year-old female, presented to the emergency department with a history of exertional dyspnea, accompanied by palpitations and chest tightness. 2D TT ECHO revealed a 60×33 mm mass with two distinct hypoechoic regions, suggestive of necrotic and hemorrhagic areas, highly mobile and protruding through the mitral valve into the left ventricle, causing significant obstruction to the flow (Figure 2). 2D, 3D TE ECHO showed the huge atrial mass be pedunculated and attached to the IAS with the central large hypoechogenic

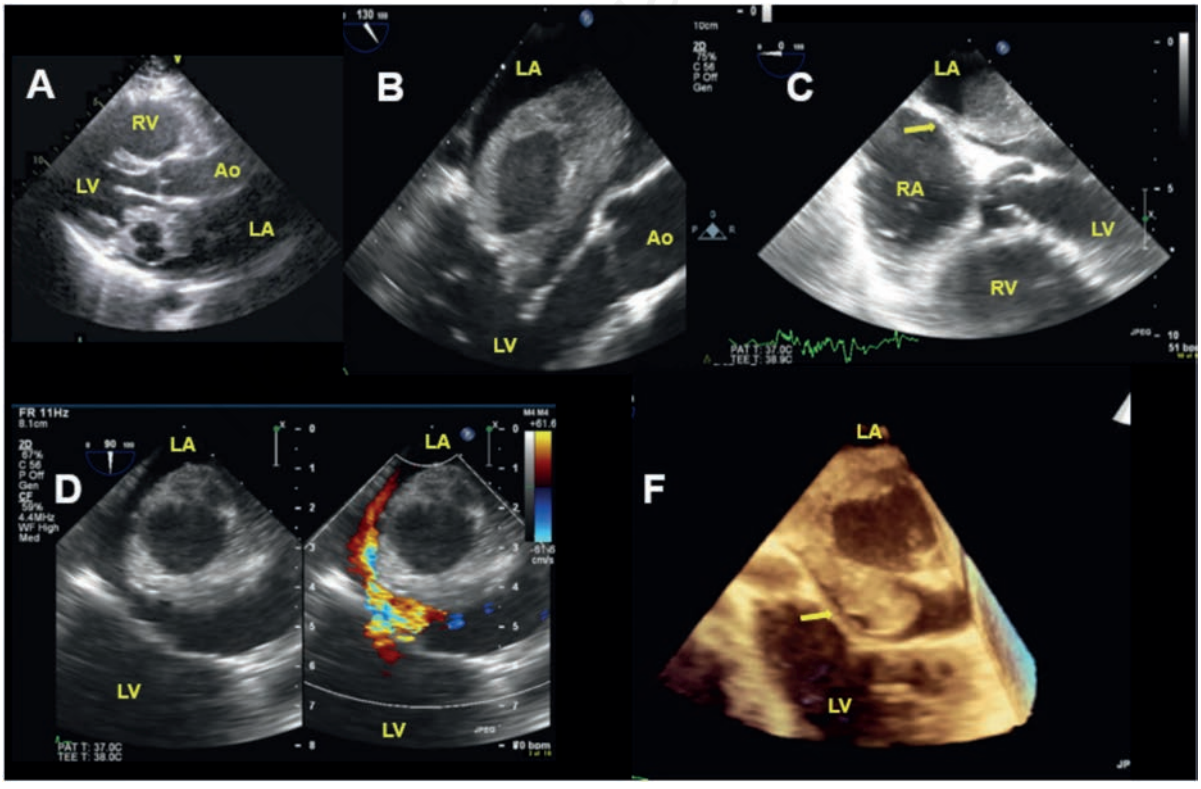

Figure 2. Case #7. A) Parasternal long axis (PLAX) view of the transthoracic echocardiography showing left atrium (LA) mass with ghost appearance obstructing mitral inflow; B) transesophageal echocardiography with mid esophageal long axis view at 130 degrees at diastole showing the mass prolapsing through the mitral valve; C) mid-esophageal 5-chamber view with the mass in LA attached to the inter-atrial septum by stalk (yellow arrow); D) transesophageal echocardiography with 2-chamber view at 90 degrees with color doppler at systole showing mitral regurgitation (MR) directed posteriorly around the mass and 3D transesophageal echocardiography image showing the mass interfering with mitral valve closure as a possible mechanism of the MR; F) PLAX, para-sternal long axis view.

area with cystic appearance, likely central hemorrhage. The patient underwent surgical removal of 4.5 cm mass, which was diagnosed in pathology to be a solid myxoma (Figure 2).

Case #8

A 47-year-old male presented with back pain and bradycardia. 2D TT ECHO revealed a left atrial mass, but the attachment was unclear. 2D 3D TE ECHO confirmed the mass as pedunculated, attached to the IAS. Cardiac MRI described a 4.2×2.5×2.6 cm mobile lobulated mass in the LA, arising above the fossa ovalis, in contact with the mitral valve but not protruding. It showed varied intensities on T1 and STIR sequences, with central hypervascularity and peripheral enhancement post-contrast, possibly due to a fibrovascular core. Surgical excision yielded a 3×4 cm mass attached to the septum. Pathology highlighted a smooth pedunculated surface with hemorrhagic nodules.

Case #9

A 71-year-old female with a history of aortic stenosis, diabetes mellitus, chronic kidney disease and severe aortic stenosis was scheduled for aortic valve replacement. At preoperative 2D TT ECHO, no LA mass was reported. Unexpectedly, pre-operative 3D TE ECHO revealed a 19×12 mm sessile mass in the LA attached to the IAS. During surgery, the atrial mass was excised, the aortic valve was replaced, and a coronary artery bypass was performed. A gross examination of the mass demonstrated gray-tan fibrous tissue, and pathology identified a myxoid lesion with fibrous stroma.

Case #10

A 39-year-old male presented with diarrhea and abdominal pain. Abdominal CT identified ulcerative colitis and an incidental hypodense, sessile, lobulated mass adhering to the LA inferior wall. Subsequent 2D TT ECHO revealed a 14×24 mm mobile mass on the IAS. 2D and 3D TE ECHO imaged a mass with heterogeneous texture and well-defined borders, with the top fimbriated edges, attached to the atrial wall. Before surgery, the patient exhibited right-sided weakness, slurred speech, and heaviness. Brain CT indicated an embolic stroke. Surgical excision revealed a 3.5×3.5 cm thrombosed mass on the LA anterolateral wall. Grossly, the mass was a brown tan and firm. Pathology described solid myxoma arranged in cords with vessels.

Case #11

A 19-year-old female with a history of double outlet right ventricle, dextro-transposition of great vessels, hypoplastic right ventricle, large inlet ventricular septal defect, and overriding TV underwent Blalock-Taussig shunt, Glenn shunt, and Fontan procedures. During her annual 2D TT ECHO, a 2×2 cm mobile mass with a short tick pedicle was identified in the right ventricular outflow tract (RVOT) below the aortic valve without sub-aortic obstruction. 2D/3D TE ECHO characterized the mass as rounded, with delineated borders, attached by a short tick pedicle in the RVOT below the aortic valve, heterogeneous without causing RVOT obstruction (Figure 3). A cardiac MRI confirmed the mass attached to the RVOT below the aortic valve with LGE. Surgical excision yielded soft red tissue. Pathology confirmed the mass as a solid myxoma, vasoformative subtype.

Case #12

An 18-year-old male who already underwent two surgical resections of myxomas, one in the LA (4 years before) and a second in the RA (3 years before), with heterozygous *PRKAR1A* gene mutation, indicative of Carney complex, was found to have by TT ECHO a recurrent right atrial mass, attached to the IAS (Figure 4). 2D and 3D TE ECHO detected a large mobile, with well-delineated margins and a heterogenous mass attached to the RA wall just anterior to the mouth of the inferior vena cava (IVC), measuring ~4×3 cm in diam-

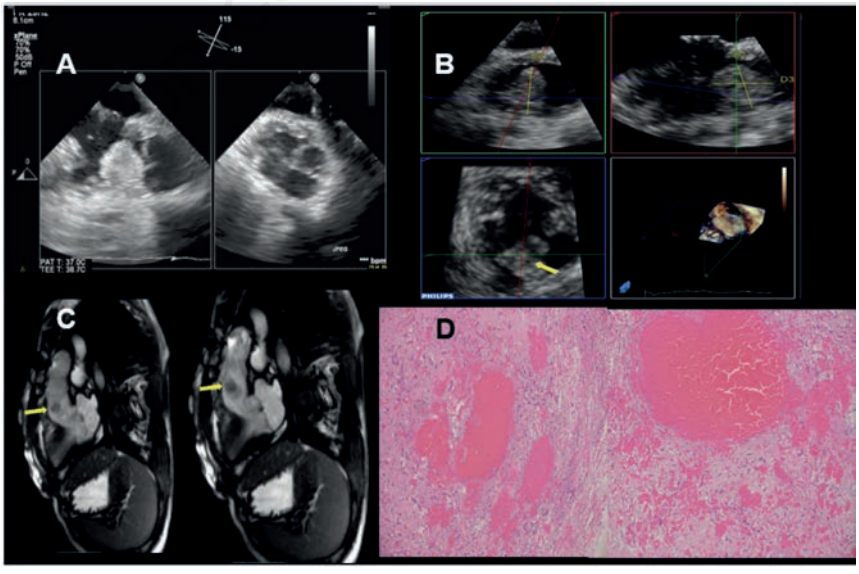

Figure 3. Case #11. A) Transesophageal echocardiography showing mass attached to the anterior right ventricular outflow tract (RVOT) just below the aortic valve; B) 2D cross-sectional views on transesophageal echocardiography 3D volume showing the attachment to the RVOT (yellow arrow); C) steady-state free precession magnetic resonance of RVOT with mass seen below aortic valve (end-diastole and systole); D) acid-mucopolysaccharide-rich myxoid matrix with polygonal stromal cells; solid mixoma vasoformative subtype.

eter and partially protruding into the TV inflow and partially obstructing the inflow of the coronary sinus. No obstruction to IVC, superior vena cava, or TV inflow was observed. CMR reported a 2.7×3.7×4.6 cm lobulated RA mass, contiguous with the TV posterior leaflet, partially extending to the atrio-caval junction and mildly intruding the IVC without causing obstruction. Imaging displayed intermediate T1, and high T2 and STIR signal intensities. Perfusion images exhibited mild heterogeneous enhancement. Surgical excision revealed a red-tan, multinodular, hemorrhagic tissue/mass coated in gelatinous material. Histopathology identified a solid myxoma with ectatic vessels, fibrin, stellate cells in a myxoid matrix, multinucleated giant cells, and hemosiderin-laden macrophages. The patient remained recurrence-free after a 3-year-follow up.

Case #13

A 48-year-old female known to have hypertension was incidentally diagnosed with LA mass during the evaluation of a breast cyst by CT scan. TT ECHO imaged a rounded shape, with a smooth surface, homogeneous, large mass (1.9×1.6 cm) attached to fossa ovalis whose type of attachment was not visualized (Figure 5). 3D/2D TE ECHO were able to better assess the morphological feature and attachment by a peduncle to the fossa ovalis; cardiac MRI showed a mobile mass attached to the fossa ovalis with LGE. Surgical excision done grossly showed: a reddish ovoid mass with a smooth surface attached by a large stump to IAS. Pathology confirmed solid tumor.

Discussion

Our series demonstrated a wide and unusual anatomical spectrum of CM. The classical morphology of the myxoma (mobile with well-delineated margins attached by a stalk to the IAS) was present in the minority of cases, with most of them being sessile. We have 17 myxomas in 13 patients with a wide variety of origins in different areas of the RA, LA, IAS, LAA, mitral valve and RVOT. The rarer and more unusual locations were RVOT in a patient with double outlet right ventricle and dextro-transposition of great vessels, LAA, and mitral valve. The texture showed a wide variety (homogeneous myocardial-like, heterogeneous with hyperechogenic areas suggestive of calcifications or hypoechoic areas consistent with intratumoral hemorrhage. The heterogeneousity was better visualized by 3D electronic sectioning. In one patient a huge size myxoma exhibited a cystic appearance with a central large hypoechogenic area found at surgery and pathology be an intratumoral hemorrhage. The size ranged from small to huge dimensions. 2D TE ECHO was shown to be able to visualize the anatomical features better than TT ECHO in particular dealing with the type of attachment. 3D TE ECHO confirmed all the findings of 2D TT ECHO but allowed for a more detailed assessment of the mass' anatomical features. In all the myxomas 3D TEE was able to correctly identify the peduncle that was not seen in 4 cases by 2D TE ECHO, and two small recurrent small myxomas were not visualized by 2D TE ECHO and by MRI.

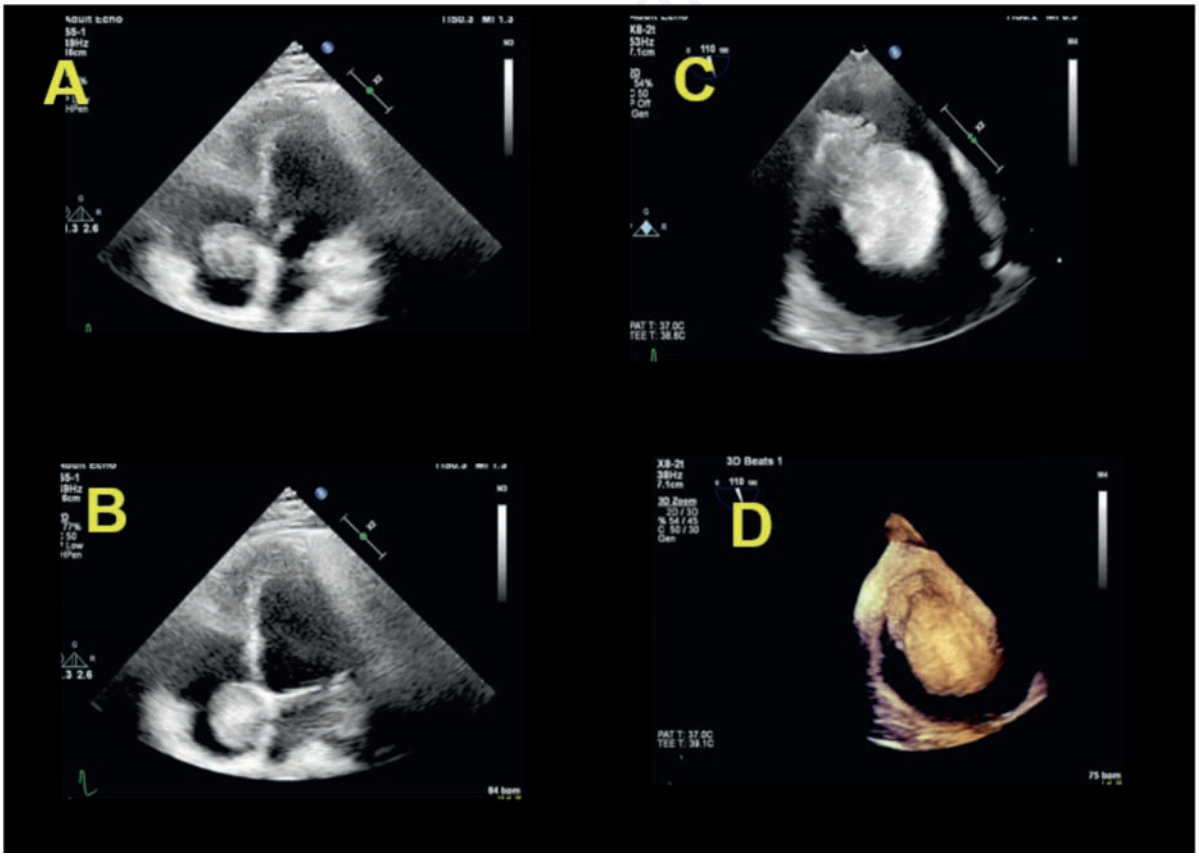

Figure 4. Case #12. A,B) Transthoracic echocardiography diastole and systole; large atrial RA mass in the right atrium (RA) that seems attached to the interatrial septum protruding into the tricuspid valve during diastole; C) 2D transesophageal echocardiography RA mass attached to the atrial wall close to the inferior vena cava (IVC) opening; D) 3D transesophageal echocardiography; enface view of the RA mass attached to the atrial wall close to the opening of IVC.

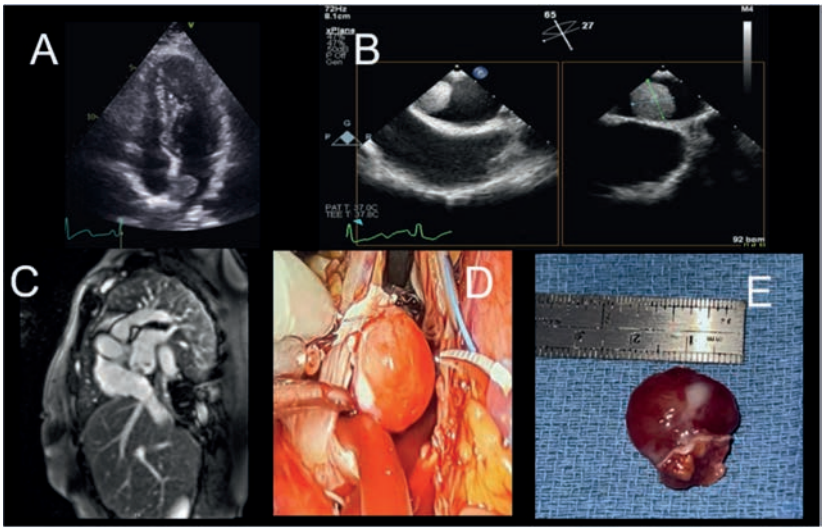

Figure 5. Case #13. A) Transthoracic echocardiography: rounded shaped, with smooth surface, homogeneous, large mass (1.9×1.6 cm) attached to fossa ovalis whose type of attachment was not visualized; B) 2D transesophageal echocardiography X plane showing a round large mass (1.9×1.6 cm) attached to fossa ovalis by a thick stalk; C) cardiac magnetic resonance showed mobile mass attached to fossa ovalis with late gadolinium enhancement; D) intraoperative picture: reddish ovoid mass smooth surface attached by large stump to the interatrial septum; E) Grossy specimen.

In two patients myxomas were papillary, one of them had embolism, attachments were atypical for location and type (one tiny peduncle on the base of IAS close to RIPV and the other sessile in the roof of the LA) and the texture was homogeneous with irregular fimbriated margins, one with fluffy appearance. One patient with solid myxoma experienced embolism, and at surgery, it was found to have a clot attached on the mobile side. Two patients had recurrence: the first was without major clinical criteria suggestive of Carney syndrome (skin, conjunctiva, and lips lentigines, subclinical hypercortisolism, and nodular thyroid changes) except for CM and no mutations of *PRKAR1A* gene. Unusual was the histology that revealed a papillary type in the first episode and a solid type with five myxomas in the recurrence. In the second case, genetic testing revealed a heterozygous *PRKAR1A* gene mutation, indicative of Carney complex associated also with a skin fibromyxoma. Even though echo has excellent sensitivity for CM diagnosis, the specificity is still modest due to a wide differential diagnosis [1-9]. MRI has a key role in the cardiac tumor imaging pathway, and it is considered the gold standard for diagnosing cardiac tumors and myxomas allowing not only the detection of the morphologic features of the intracardiac masses but also the evaluation of various parameters including tissue characterization, edema, iron content, perfusion, enhancement, and fat saturation/suppression. However, it also presents some technical limitations and might not always detect anatomical features like tiny stalks [16,17]. In our series, we were able to clearly reveal the anatomical characteristics. In only one case, it was not able to detect two small myxomas likely due to the small size and the unusual location [17].

The differential diagnosis is challenging because the myxomas can be misdiagnosed with other cardiac tumors in particular with fibroelastomas [5], and hemangiomas [22], where the MRI findings are similar to a myxoma with vascular neoformation as in two of our cases and also clot particularly in unusual location [22] or tuberculoma [23,24].

In the context of CM imaging, 3D TE ECHO, providing detailed real-time anatomical imaging and unique electronic scanning, may play an emerging role as a key adjunctive modality, especially when anatomical clarity is lacking with 2D ECHO and advanced surgical planning is required [10-19]. Furthermore, the use of anatomical imaging and an anatomy-based vocabulary, which is better understood by cardiac surgeons and multimodality imagers, positions 3D TE ECHO as the echocardiographic modality that can enhance communication within the Heart Team [10,11]. By bridging the gap between 2D ECHO and anatomy and adding more detailed information on the morphologic features, its utilization could represent a missing link in myxoma imaging [10-19].

Conclusions

Our study showed that myxomas have a wide anatomical spectrum beyond the typical feature making the diagnosis challenging in the clinical arena. A detailed multimodality imaging of the anatomical features is paramount in the differential diagnosis among cardiac masses and the histological types of myxomas. 3D TE ECHO has shown to be a valuable additional imaging technique able to add important morphologic information useful in clinical decision-making and in surgical planning.

References

1. Bjessmo S, Ivert T. Cardiac myxoma: 40 years' experience in 63 patients. Ann Thorac Surg 1997;63:697-700.
2. Centofanti P, Di Rosa E, Deorsola L, et al. Primary cardiac tumors: early and late results of surgical treatment in 91 patients. Ann Thorac Surg 1999;68:1236-41.
3. Poterucha TJ, Kochav J, O'Connor DS, Rosner GF. Cardiac tumors: clinical presentation, diagnosis and management. Curr Treat Opt Oncol 2019;20:66.
4. Tyebally S, Chen D, Bhattacharyya S, et al. Cardiac tumors: JACC CardioOncology state-of-the-art review. JACC Cardio Oncol 2020;2:293-311.

5. El Sabbagh AD, Al-Hijji MA, Thaden JJ, et al. Cardiac myxoma: the great mimicker. JACC Cardiovasc Imaging 2017;10:203-6.
6. Kalçık M, Bayam E, Güner A, et al. Evaluation of the potential predictors of embolism in patients with left atrial myxoma. Echocardiography 2019;36:837-43.
7. Koritnik P, Pavsic N, Bervar M, Prokselj K. Echocardiographic characteristics of cardiac myxoma. Eur Heart J 2021;42:ehab 724.0146.
8. Mankad R, Herrmann J. Cardiac tumors: echo assessment. Echo Res Pract 2016;3:R65-77.
9. Parato VM, Nocco S, Alunni G, et al. Imaging of cardiac masses: an updated overview. J Cardiovasc Echogr 2022;32:65-75.
10. Lang RM, Addetia K, Narang A, Mor-Avi V. 3-dimensional echocardiography: latest developments and future directions. JACC Cardiovasc Imaging 2018;11:1854-78.
11. Faletra FF, Agricola E, Flachskampf FA, et al. Three-dimensional transoesophageal echocardiography: how to use and when to use - a clinical consensus statement from the European Association of Cardiovascular Imaging of the European Society of Cardiology. Eur Heart J Cardiovasc Imaging 2023;24:e119-197.
12. Galzerano D, Kinsara AJ, Di Michele S, et al. Three dimensional transesophageal echocardiography: a missing link in infective endocarditis imaging? Int J Cardiovasc Imaging 2020;36:403-13.
13. Khairnar P, Hsiung MC, Mishra S, et al. The ability of live three-dimensional transesophageal echocardiography to evaluate the attachment site of intracardiac tumors. Echocardiography 2011;28:1041-5.
14. Tolstrup K, Shiota T, Gurudevan S, et al. Left atrial myxomas: correlation of two-dimensional and live three-dimensional transesophageal echocardiography with the clinical and pathologic findings. J Am Soc Echocardiogr 2011;24:618-24.
15. Zaragoza-Macias E, Chen MA, Gill EA. Real time three-dimensional echocardiography evaluation of intracardiac masses. Echocardiography 2012;29:207-19.
16. Galzerano D, Pragliola C, Al Admawi M, et al. The role of 3D echocardiographic imaging in the differential diagnosis of an atypical left atrial myxoma. Monaldi for Chest Dis 2018;88:906.
17. Al Sergani R, Alamr B, Al Admawi M, et al. Three dimensional echocardiographic imaging of multiple recurrent myxomas. Monaldi for Chest Dis 2020;90:1188.
18. Khairnar P1, Hsiung MC, Mishra S et al. The ability of live three-dimensional transesophageal echocardiography to evaluate the attachment site of intracardiac tumors. Echocardiography 2011;28:1041-5.
19. Espinola-Zavaleta N, Lozoya-Del Rosal JJ, Colin-Lizalde L, Lupi-Herrera E. Left atrial cardiac myxoma. Two unusual cases studied by 3D echocardiography. BMJ Case Rep 2014;2014: bcr2014205938.
20. Abbas A, Garfath-Cox KAG, Brown IW, et al. Cardiac MR assessment of cardiac myxomas Br J Radiol 2015;88:1045.
21. Basso C, Buser PT, Rizzo S, et al. Benign cardiac tumors. In: V. Ferrari, ed. EACVI textbook of cardiovascular magnetic resonance. Oxford: Oxford University Press; 2018. pp 469-73.
22. Galzerano D, Eltayeb A, Alamri S, et al. A ping pong ball in the left ventricle. J Cardiothorac Vasc Anesth 2023;37:2153-6.
23. Alamri F, Eltayeb A, Hamad A, et al. A native mitral valve mass beyond imagination. Monaldi Arch Chest Dis 2023;94:2649.
24. Pergola V, Al-Admawi M, Fadel B, Di Salvo G. An unusual cardiac mass: echocardiography, computed tomography, and magnetic resonance imaging. J Cardiol Cases 2016;13:143-5.